

# Embryonic and Larval Expression of Zebrafish Voltage-Gated Sodium Channel $\alpha$ -Subunit Genes

Alicia E. Novak,<sup>1</sup> Alison D. Taylor,<sup>1</sup> Ricardo H. Pineda,<sup>1</sup> Erika L. Lasda,<sup>2</sup> Melissa A. Wright,<sup>1,3</sup> and Angeles B. Ribera<sup>1,3\*</sup>

Whereas it is known that voltage-gated calcium channels play important roles during development, potential embryonic roles of voltage-gated sodium channels have received much less attention. Voltage-gated sodium channels consist of pore-forming  $\alpha$ -subunits ( $\text{Na}_v1$ ) and auxiliary  $\beta$ -subunits. Here, we report the embryonic and larval expression patterns for all eight members of the gene family (*scna*) coding for zebrafish  $\text{Na}_v1$  proteins. We find that each *scna* gene displays a distinct expression pattern that is temporally and spatially dynamic during embryonic and larval stages. Overall, our findings indicate that *scna* gene expression occurs sufficiently early during embryogenesis to play developmental roles for both muscle and nervous tissues. *Developmental Dynamics* 235:1962–1973, 2006. © 2006 Wiley-Liss, Inc.

**Key words:** zebrafish; *SCNA* gene; electrical signaling;  $\text{Na}_v1$  protein; skeletal muscle; cardiac muscle; nervous system; spinal cord

Accepted 7 March 2006

## INTRODUCTION

Vertebrate development relies upon multiple forms of inter- and intracellular communication. One form of intracellular communication, electrical excitability, involves the concerted activity of several different types of voltage-gated ion channels, such as calcium, potassium, and sodium voltage-gated channels (Hille, 2001). Voltage-gated calcium channels play roles in a diverse range of early developmental processes, including mesodermal patterning and neural induction (Moreau et al., 1994; Drean et al., 1995; Leclerc et al., 1995, 1997, 2000; Palma et al., 2001; Wallingford et al.,

2001). At later stages, voltage-gated calcium channels also regulate differentiation of cardiac tissue and neuronal migration (Moran, 1991; Komuro and Rakic, 1992; Rottbauer et al., 2001).

Previous studies examining the roles of ion channels during early embryonic development have focused largely on voltage-gated calcium channels (but see Rutenberg et al., 2002). However, in addition to calcium channels, voltage-gated sodium channels ( $\text{Na}_v1$ ) initiate electrical signals. Furthermore, at least in mammals, sodium channel gene (*SCNA*) gene expression has been detected in embryonic and neonatal stages (Table 1 and references therein).

The nine different mammalian *SCNA* genes differ with respect to expression patterns as well as functional properties (e.g., sensitivity to tetrodotoxin; Table 1). Studies on human diseases, known as ion channelopathies, have revealed the essential roles of some mammalian *SCNA* genes. A mutation in the human *SCN1A* gene results in a childhood disease known as generalized epilepsy with febrile seizures plus (GEFS+; Escayg et al., 2001). Furthermore, mutations in the *SCN1A* and *SCN2A* have been found in individuals with familial forms of autism (Weiss et al., 2003). Despite that these diseases affect children, the

<sup>1</sup>Department of Physiology & Biophysics, UCDHSC at Fitzsimons, Aurora, Colorado

<sup>2</sup>Department of Biochemistry, UCDHSC at Fitzsimons, Aurora, Colorado

<sup>3</sup>Medical Scientist Training Program, UCDHSC, Denver, and Neuroscience Program, UCDHSC at Fitzsimons, Aurora, Colorado  
Grant sponsor: National Institutes of Health (National Institute of Neurological Disease and Stroke); Grant number: R01 NS038937; Grant number: P30 NS048154.

\*Correspondence to: Angeles B. Ribera, Department of Physiology & Biophysics, Mail Stop 8397, UCDHSC at Fitzsimons, P.O. Box 6511, Aurora, CO 80045. E-mail: angie.ribera@uchsc.edu

DOI 10.1002/dvdy.20811

Published online 13 April 2006 in Wiley InterScience (www.interscience.wiley.com).

roles of SCNA genes and Na<sub>v</sub>1 proteins during development have received comparatively little attention.

One zebrafish mutant, *macho* (*mao*), is touch-insensitive and behaviorally blind due to a reduction of voltage-gated sodium current in Rohon-Beard (RB) sensory neurons and retinal ganglion cells (Granato et al., 1996; Ribera and Nüsslein-Volhard, 1998; Neuhauss et al., 1999; Gnügge et al., 2001). Even though sodium current is reduced in these neurons, the *mao* gene does not show linkage to any zebrafish *scna* gene (Novak et al., 2006; Geisler and Neuhauss, personal communication). Of interest, in *mao* mutants, both RB and retinal ganglion cells differentiate abnormally, suggesting developmental roles for sodium channels. For example, retinal ganglion axons display incorrect mapping to the tectum (Granato et al., 1996; Gnügge et al., 2001). Similarly, RB cells are normally rapidly eliminated by programmed cell death but survive longer in *mao* mutants (Svoboda et al., 2001).

As a first step toward investigating developmental roles of SCNA genes, we determined their expression patterns in a vertebrate system that facilitates embryonic analyses (Westerfield, 1995; Nüsslein-Volhard and Dahm, 2002). The zebrafish embryo develops externally, thus avoiding experimental complications imposed by the intra-uterine development of mammals. Furthermore, large numbers of embryos are produced by single pair breedings. Development of the embryo and larva occurs quickly, and, by 5 days postfertilization (dpf), the vast majority of internal and external organs and structures have reached maturity. The embryo is relatively transparent, allowing repeated observation in the same specimen of internal structures without dissection. Additional advantages include the vast array of genetic, molecular, cellular, and physiological studies that are possible in this system as well as the ability to perform large-scale mutagenesis screens (e.g., *mao*) and to knock down genes of interest using antisense morpholinos (Westerfield, 1995; Nüsslein-Volhard and Dahm, 2002; Novak and Ribera, 2005).

In zebrafish, the *scna* family consists of four sets of duplicated genes:

*scn1Laa* & *scn1Lab*, *scn4aa* & *scn4ab*, *scn5Laa* & *scn5Lab*, and *scn8aa* & *scn8ab* (Novak et al., 2006). Although there are several multimember gene families in zebrafish that contain duplicated sets of genes (e.g., *hox* genes; Amores et al., 1998), the *scna* family is unusual in that all of the duplicates have been retained. Typically, when duplicated genes are retained in a species (1) new functions evolve, or (2) the functions of the ancestral gene are partitioned (Postlethwait et al., 2004). Subfunction partitioning can occur at temporal, spatial, or quantitative levels (Postlethwait et al., 2004). Comparisons of the expression patterns of the four sets of duplicated *scna* genes might provide insights regarding why all eight have been retained, unlike other duplicated gene families (e.g., *hox*).

Prior work has indicated that *scn8aa* is expressed embryonically in the nervous system (Tsai et al., 2001). However, the embryonic and larval expression patterns of the other seven *scna* genes have not yet been reported. Furthermore, it is not known whether muscle as well neural tissues express *scna* genes during embryogenesis. The latter is a question of evolutionary interest because ancestral SCNA genes are thought to have been expressed in a restricted manner, each limited to one type of excitable tissue (for reviews, see Plummer and Meisler, 1999; Goldin, 2002).

Here, we report that all eight zebrafish *scna* genes are expressed during embryonic and larval development. Furthermore, each *scna* gene displays a characteristic spatially and developmentally regulated expression pattern. Whereas some *scna* genes display neural-specific expression, as reported previously for *scn8aa*, others display muscle-specific patterns between 10 and 120 hours postfertilization (hpf). In addition, some *scna* genes are expressed in both neural and muscle tissues. Although one *scna* gene, *scn8ab*, displays an expression pattern that is entirely contained within that of *scn8aa*, analysis of alternative splicing revealed novel properties. Furthermore, only one gene, *scn8aa*, is expressed in the same neurons that show reduced sodium currents in the *mao* mutant. Overall, our results indicate that *scna* genes are

expressed at the right time and place to contribute to early electrical events that regulate embryonic development of vertebrate neural and muscle tissue.

## RESULTS AND DISCUSSION

### Design of *scna* Isotype-Specific In Situ Hybridization Probes

Developmental expression patterns of zebrafish *scna* genes were analyzed using whole-mount in situ hybridization in embryos ranging in age from 2 to 120 hpf. To develop *scna* isotype-specific probes, we identified regions that diverged significantly among the eight zebrafish *scna* genes. SCNA genes typically share high sequence identity across their transmembrane repeat regions. Furthermore, in zebrafish, members of a duplicated *scna* gene pair display even higher nucleotide and amino acid identity (Novak et al., 2006). For example, the coding regions of *scn8aa* and *scn8ab* are 88% identical at the predicted amino acid level. Thus, we were concerned that in situ hybridization probes for one member of a duplicated gene pair (e.g., *scn8aa*) might cross-hybridize to the other member of the pair (e.g., *scn8ab*).

Typically, the most divergent regions of *scna* genes are the domains that code for (1) the linkers between membrane-spanning repeats (I, II, III, and IV), (2) the large carboxyl-terminus, or (3) 3'-untranslated regions (UTRs; Fig. 1). By focusing on these regions, we were able to design in situ hybridization probes that recognized regions that differed as much as 80% between *scna* genes (Table 1). Importantly, the probe sequences that had the most divergent sequences were for the duplicated genes that are overall most similar to each other, *scn8aa* and *scn8ab* (88% identity; Table 1; Novak et al., 2006).

### Zebrafish *scn1La* Duplicated Genes Are Expressed Exclusively in the Nervous System

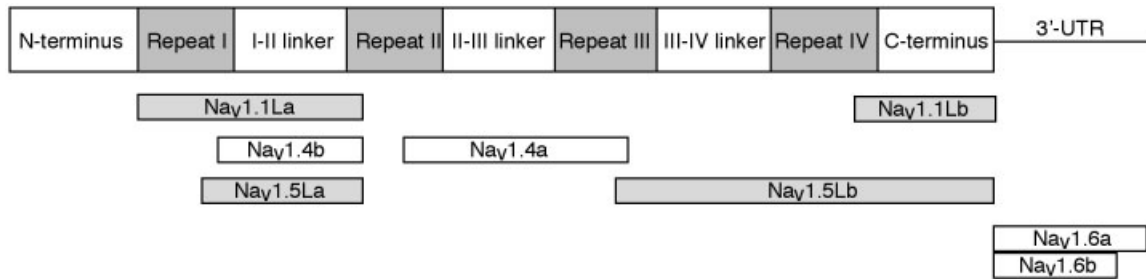
*Scn1Laa* and *scn1Lab* sequences display 67% predicted amino acid identity. Among the four sets of zebrafish

TABLE 1. Mammalian Scn Gene Expression Patterns<sup>a</sup>

Mammalian gene (protein) TTXs/r	Brain	Spinal cord	Retina	PNS	Skeletal muscle	Cardiac muscle	<i>Danio rerio</i> co-orthologues (protein names)	Ref <sup>b</sup>
<i>SCN1A</i> (Na <sub>v</sub> 1.1) TTXs	Present in neonate, persists in adult	Present in neonate and adult; in sensory and motor neurons	Adult	Present in neonate and adult	- - -	Present in neonate and adult in T-tubules	<i>scn1Laa/scn1Llab</i> (Na <sub>v</sub> 1.1La/Na <sub>v</sub> 1.1Lb)	1, 2, 3, 4, 5
<i>SCN2A</i> (Na <sub>v</sub> 1.2) TTXs	Present in embryo, peaks neonatally, persists in adult	Present in embryo, peaks in neonate, persists in adult; in motor neurons	Adult	Present in embryo, neonate, and adult	- - -	Present in neonate and adult	<i>scn1Laa/scn1Llab</i> (Na <sub>v</sub> 1.1La/Na <sub>v</sub> 1.1Lb)	1, 2, 3, 4, 5
<i>SCN3A</i> (Na <sub>v</sub> 1.3) TTXs	Present in embryo, peaks neonatally, persists in adult	Present in embryo, peaks in neonate, persists in adult	Adult	Present in embryo, neonate, and adult	- - -	Present in neonate and adult in T-tubules	<i>scn1Laa/scn1Llab</i> (Na <sub>v</sub> 1.1La/Na <sub>v</sub> 1.1Lb)	1, 2, 3, 4, 5
<i>SCN4A</i> (Na <sub>v</sub> 1.4) TTXs	Not found in adult	- - -	- - -	- - -	Abundant	- - -	<i>scn4aaa/scn4ab</i> (Na <sub>v</sub> 1.4a/Na <sub>v</sub> 1.4b)	6, 7, 8, 9
<i>SCN5A</i> (Na <sub>v</sub> 1.5) TTXr	Limbic system of neonate and adult	- - -	- - -	- - -	Neonate and after denervation	Abundant in adult in intercalated disks; splice variant "a" in embryo	<i>scn5Laa/scn5Llab</i> (Na <sub>v</sub> 1.5La/Na <sub>v</sub> 1.5Lb)	6, 9, 10, 11, 12, 13
<i>SCN8A</i> (Na <sub>v</sub> 1.6) TTXs	Present in embryo, peaks neonatally, persists in adult	Present in embryo, peaks in neonate, persists in adult; in motor and sensory neurons and glia	Adult	Present in embryo, neonate, and adult	- - -	Present in neonate and adult; localized to T-tubules	<i>scn8aaa/scn8ab</i> (Na <sub>v</sub> 1.6a/Na <sub>v</sub> 1.6b)	4, 5, 14, 15, 16
<i>SCN9A</i> (Na <sub>v</sub> 1.7) TTXs	Low level/absent	Low level/absent	Absent	Present in neonate and adult	- - -	- - -	<i>scn1Laa/scn1Llab</i> (Na <sub>v</sub> 1.1La/Na <sub>v</sub> 1.1Lb)	17
<i>SCN10A</i> (Na <sub>v</sub> 1.10) TTXr	Absent	Absent	- - -	Present in embryo, neonate and adult	- - -	- - -	<i>scn5Laa/scn5Llab</i> (Na <sub>v</sub> 1.5La/Na <sub>v</sub> 1.5Lb)	5, 18, 19, 20
<i>SCN11A</i> (Na <sub>v</sub> 1.11) TTXr	Absent	Adult; in glia	- - -	Present in embryo, neonate, and adult	- - -	- - -	<i>scn5Laa/scn5Llab</i> (Na <sub>v</sub> 1.5La/Na <sub>v</sub> 1.5Lb)	21

<sup>a</sup>—, not examined; TTX, tetrodotoxin; PNS, s, sensitive; r, resistant; Ref, References.

<sup>b</sup>1, Noda et al., 1986; 2, Beckh et al., 1989; 3, Black et al., 1994; 4, Black et al., 1996; 5, Felts et al., 1997; 6, Cooperman et al., 1987; 7, Trimmer et al., 1989; 8, Trimmer et al., 1990; 9, Yang et al., 1991; 10, Gellens et al., 1992; 11, Donahue et al., 2000; 12, Hartmann et al., 1999; 13, Renganathan et al., 2002; 14, Krzemien et al., 2000; 15, Schaller et al., 1995; 16, Schaller and Caldwell, 2000; 17, Toledo-Aral et al., 1997; 18, Akopian et al., 1996; 19, Akopian et al., 1999a; 20, Akopian et al., 1999b; 21, Dib-Hajj et al., 1998.



**Fig. 1.** In situ hybridization probes recognize regions of *scna* genes coding for divergent regions. The general organization of a voltage-gated sodium channel ( $\text{Na}_v1$ ) protein is shown at the top. The sequence predicts four transmembrane repeat regions (I, II, III, IV; dark gray) separated by cytoplasmic linker regions (white). The amino and carboxyl termini are also thought to be cytoplasmic (white). For *scn1Laa*, *scn1Lab*, *scn4aa*, *scn4ab*, *scn5Laa*, and *scn5Lab*, in situ hybridization probes recognize divergent sequences within regions coding for linkers or carboxyl termini of the respective  $\text{Na}_v1$  proteins. However, because of the greater similarity between *scn8aa* and *scn8ab*, highly divergent sequences are only found within the 3'-untranslated regions (3'-UTRs; line).

**TABLE 2. In Situ Hybridization Probe Design and Specificity<sup>a</sup>**

Gene	Length (bp)	Nucleotide identity (%)	
		To duplicate	To other $\text{Na}_v$
<i>scn1Laa</i>	1,900	57	48–51
<i>scn1Lab</i>	765	52	42–56
<i>scn4aa</i>	812	59	50–57
<i>scn4ab</i>	910	51	39–47
<i>scn5Laa</i>	1,111	52	43–47
<i>scn5Lab</i>	1,800	71	57–61
<i>scn8aa</i>	655	20	nd
<i>scn8ab</i>	450	20	nd

<sup>a</sup>nd, not determined (3' untranslated region sequences of other *scna* genes have not been identified).

*scna* duplicated gene pairs, they are the least similar to each other. Previous phylogenetic analyses have indicated that *scn1Laa* and *scn1Lab* are evolutionarily related to the mammalian *SCN1A*, *SCN2A*, *SCN3A*, and *SCN9A* genes (Novak et al., 2006; Table 2). The four mammalian genes reside in a cluster on a single chromosome in both humans and mice (Goldin, 2002). The expression patterns of these four mammalian *SCNA* genes differ substantially. For example, *SCN9A* expression is restricted to the peripheral nervous system, whereas those of *SCN1A*, *SCN2A*, and *SCN3A* occur both centrally as well as in the periphery (Table 1, and references therein). With respect to development, *SCN1A* gene expression is not detected until postnatal stages. In contrast, *SCN2A* and *SCN3A* gene expression is found in the embryo (Table 1). *SCN9A* expression begins during postnatal stages (Toledo-Aral et al., 1997).

In zebrafish, at 24 hpf, RB and trigeminal ganglion neurons display *scn1Laa* mRNA (Fig. 2A–D). At 48 hpf, expression is still present in the trigeminal ganglion and to a lesser extent in RB cells (Fig. 2E–H). These results indicate that *scn1Laa* expression is restricted to the dorsal or sensory nervous system.

In contrast, the *scn1Lab* transcripts are detected in the ventral nervous system. Expression is first detected at 24 hpf in ventral regions of the hindbrain and spinal cord (Fig. 3A–E). In the hindbrain, the expression pattern suggests branchiomotor neurons (e.g., Higashijima et al., 2000; Cooper et al., 2005). At 48 hpf, mRNA expression becomes more diffuse in the brain (Fig. 3F–J). Expression in the hindbrain is no longer restricted to discrete ventral compartments (Fig. 3F,G). Instead, expression is more widespread, extending dorsally within the hindbrain and rostrally (Fig. 3F,G). In spinal cord, the in situ hy-

bridization signal is detected by epifluorescent but not brightlight illumination (Fig. 3H–J). However, unlike the situation in more rostral regions of the nervous system, expression continues to display a ventral restriction.

The results indicate that transcripts coding for *scn1Laa* and *scn1Lab* are both restricted to the nervous system. However, the expression patterns for the two genes are not overlapping. *scn1Laa* mRNA localizes to dorsal, sensory regions in contrast to the ventral disposition of *scn1Lab* transcripts. In this regard, the *scn1Lab* expression resembles that of mammalian *SCN1A*, *SCN2A*, and *SCN3A* that are expressed in the CNS. In contrast, *scn1Laa* is reminiscent of the peripherally expressed *SCN9A*. These results raise the possibility that, as the neural crest evolved in vertebrates, duplication of the common ancestor to *SCN1A*, *SCN2A*, *SCN3A*, *SCN9A*, *scn1Laa*, and *scn1Lab* allowed partitioning of expression between the central and peripheral nervous systems.

### *Scn4aa* and *Scn4ab* Gene Expression

Zebrafish *scn4aa* and *scn4ab* genes are most similar to the mammalian *SCN4A* gene (Novak et al., 2006). In mammals, *SCN4A* is expressed almost exclusively in skeletal muscle (Trimmer et al., 1989). Furthermore, *SCN4A* expression occurs embryonically during maturation of neuromuscular transmission (Cooperman et al., 1987; Trimmer et al., 1990).

Similar to the *scn1La* duplicated genes, *scn4aa* and *scn4ab* are expressed in nonoverlapping patterns.

At 24 hpf, *scn4aa* mRNA is barely present in the embryo (Fig. 4A). At 60 hpf, *scn4aa* transcripts localize to the anterior mesoderm surrounding the eye (Fig. 4B). In addition, expression is detected in pharyngeal muscle and pectoral fin (Fig. 4B–F).

In contrast, *scn4ab* transcripts are detected much earlier. At 10 hpf, expression is detected in both anterior and posterior mesoderm (Fig. 5A,B). Transcripts are also detected as early as the two-cell stage by *in situ* hybridization and reverse transcriptase-polymerase chain reaction (RT-PCR; not shown), indicating maternal expression. Consistent with this finding, voltage-gated sodium currents have been recorded from ascidian eggs (Hice and Moody, 1988). At 24 hpf, *scn4ab* expression is present in the developing trunk somites (Fig. 5C,D). At 60 hpf, *scn4ab* mRNA is still present in the somites (Fig. 5E,F).

Thus, the *scn4a* gene duplicates are expressed in mesodermal tissues. However, the expression patterns differ substantially within the mesoderm as well as developmentally. *Scn4aa* mRNA is found in head and pharyngeal muscle. In contrast, *scn4ab* is initially a maternal transcript, then found in presomitic mesoderm, and later present in trunk somites.

### ***Scn5Laa* and *Scn5Lab* Gene Expression**

Even though the primary sequences of zebrafish *scn5Laa* and *scn5Lab* show highest identity to mammalian *SCN5A*, the zebrafish genes are phylogenetically equally related to *SCN5A*, *SCN10A*, and *SCN11A* (Novak et al., 2006). In mammals, *SCN5A* is primarily expressed in cardiac tissue (Rogart et al., 1989; Gellens et al., 1992). Additionally, it is expressed transiently during neonatal periods in skeletal muscle and up-regulated after denervation (Kallen et al., 1990; Trimmer et al., 1990; Gellens et al., 1992). Of interest, neural expression of *SCN5A* has been detected, both centrally in the limbic system as well as peripherally in embryonic dorsal root ganglion neurons during early embryogenesis (Hartmann et al., 1999; Donahue et al., 2000; Renganathan et al., 2002). Mammalian *SCN10A* and *SCN11A* transcripts are primarily expressed in the periphery in nociceptive

dorsal root ganglion neurons both embryonically and during adult stages (Akopian et al., 1996, 1999a,b; Felts et al., 1997; Dib-Hajj et al., 1998).

At 24 hpf, *scn5Laa* mRNA is detected in regions associated with the developing heart tube (Fig. 6A, arrows). At 48 hpf, transcripts are present diffusely in dorsal regions of the midbrain and hindbrain (Fig. 6C). At 60 hpf, expression is present within rostral regions of the nervous system (Fig. 6D,E).

In contrast, *scn5Lab* expression is detected transiently at 19 hpf in trunk somites (Fig. 7A–D). By 30 hpf, somitic expression disappears and transcripts are now detected in ventral spinal cord (Fig. 7E–G). At 60 hpf, low levels of expression are detected in the developing lateral line, in regions associated with rami of the anterior and posterior lateral line nerves (Fig. 7I, arrows; see Fig. 1 of Raible and Kruse, 2000).

These data indicate that *scn5Laa* and *scn5Lab* transcripts are found within both nervous and muscle tissue. This finding contrasts with the restricted neural and mesodermal expression patterns of the *scn1La* and *scn4a* duplicates, respectively. Furthermore, even though *scn5Laa* and *scn5Lab* transcripts localize to both neurons and muscle, the expression patterns are nonoverlapping. However, neither *scn5Laa* nor *scn5Lab* is detected in neurons thought to be involved in nociception, in contrast to *SCN10A* and *SCN11A*. Surprisingly, transcripts of neither *scn5Laa* nor *scn5Lab* are detected in the larval heart by standard whole-mount *in situ* hybridization methods.

### **RT-PCR Analysis of *Scn5la* Gene Expression in Larval Cardiac Tissue**

*Scn5Laa* and *scn5Lab* are evolutionarily related to the mammalian *SCN5A* gene that codes for the principal cardiac sodium channel (Rogart et al., 1989; Gellens et al., 1992). However, our *in situ* hybridization studies did not detect either *scn5Laa* or *scn5Lab* expression in larval cardiac tissue (Fig. 6). It is possible that the endogenous autofluorescence of cardiac tissue and neighboring yolk (e.g., Fig. 4F) could interfere with detected of the fluorescent Fast

Red reaction product. To avoid this problem, we used an alternative approach and analyzed expression in RNA isolated from cardiac tissue dissected from larvae. RT-PCR analysis of 72 hpf cardiac tissue RNA reveals expression of both *scn5Laa* and *scn5Lab* (Fig. 8).

### ***Scn8aa* and *scn8ab* Gene Expression**

Among the *scna* duplicated gene pairs, *scn8aa* and *scn8ab* share the highest sequence identity (Novak et al., 2006). Nonetheless, because both have been retained in zebrafish, we expected their expression patterns to be non-overlapping, as we found for the three other *scna* duplicated gene pairs (Figs. 2–7).

Phylogenetically, *scn8aa* and *scn8ab* are related to the mammalian gene *SCN8A* (Novak et al., 2006). *SCN8A* is expressed broadly throughout the central and peripheral nervous systems during early embryogenesis (Schaller et al., 1995; Krzemien et al., 2000; Schaller and Caldwell, 2000). Previous work has shown that zebrafish *scn8aa* mRNA expression begins early (16 hpf) and occurs in many regions of both the central and peripheral nervous systems (Tsai et al., 2001). However, the probe used for the previous studies recognized a portion of the sequence coding for the highly conserved carboxyl-terminus in addition to the divergent 3'-UTR region. At the time, *scn8ab* had not been identified and its existence probably not suspected based upon mammalian SCNA gene phylogeny (Plummer and Meisler, 1999; Goldin, 2002). To avoid cross-hybridization to *scn8ab*, we limited our probe to 3'-UTR sequence (Fig. 1; Table 1), a region that is only 20% identical between *scn8aa* and *scn8ab*. Nonetheless, our *scn8aa* *in situ* hybridization results largely agree with those of Tsai et al. (2001). Expression begins early in RB cells and the trigeminal ganglion (Fig. 9A–D). One day later at 48 hpf, expression becomes more widespread in both the spinal cord and more rostral regions of the central nervous system (Fig. 9E–H). In contrast to *scn1La* genes, *scn8aa* transcripts are found in both dorsal as well as ventral regions of the nervous system. By 60 hpf, transcripts are found in the retina, otic vesicle,

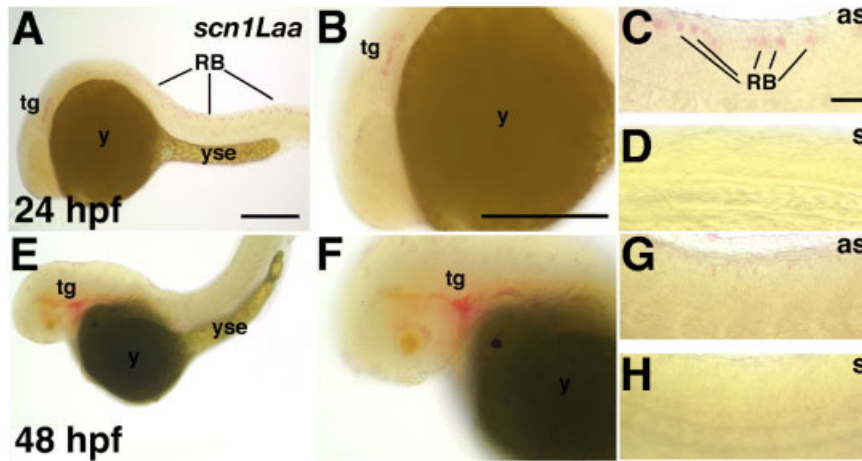


**Fig. 2.** *Scn1Laa* is expressed in sensory neurons of the peripheral nervous system and Rohon-Beard (RB) cells. **A–D:** At 24 hours postfertilization (hpf), *scn1Laa* mRNA is detected in the trigeminal ganglion and RB cells. **A:** A low-magnification view reveals expression in an anterior domain caudal to the eye and in RB cells throughout the spinal cord. **B:** At higher magnification, the anterior expression domain is recognized as the developing trigeminal ganglion migrating rostrally toward the eye. **C:** The posterior expression is found in RB cells of the spinal cord. **D:** The sense probe (s) does not reveal a signal under the same conditions used for the antisense probe (as). **E–H:** At 48 hpf, in situ hybridization signals are stronger in the trigeminal ganglion but weaker posteriorly in the spinal cord. **E,F:** At 48 hpf, the trigeminal ganglia have migrated to their characteristic position just caudal to the eye and continue to express *scn1Laa*. **G:** At 48 hpf, dorsal RB cells continue to express *scn1Laa* transcripts. **H:** The sense probe reveals no hybridization signal. as, antisense probe; n, notochord; RB, Rohon-Beard cell; s, sense probe; tg, trigeminal ganglion; yse, yolk sac extension. In this and subsequent figures, whole-mount photos are oriented with anterior to the left and dorsal up. Scale bars = 250  $\mu$ m in A (applies to A,E), 100  $\mu$ m in B (applies to B,F), 100  $\mu$ m in C (applies to C,D,G,H).

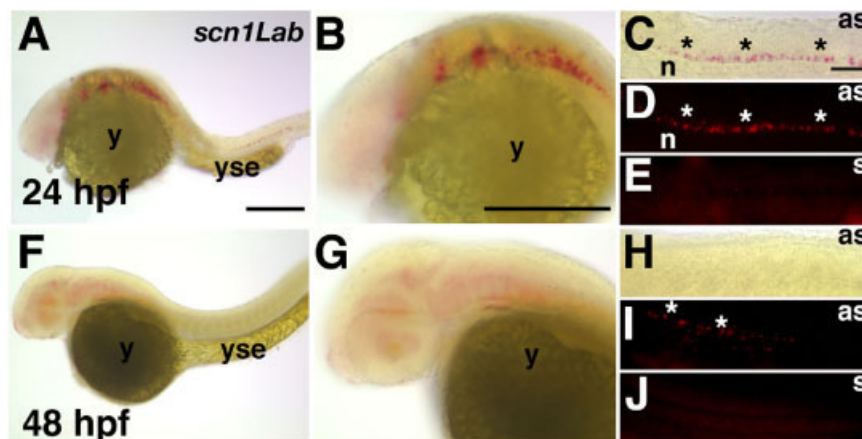


**Fig. 3.** *Scn1Lab* expression is restricted to the central nervous system. **A–E:** At 24 hours postfertilization (hpf), *scn1Lab* transcripts are detected in ventral regions of the hindbrain and spinal cord. **A:** A low-magnification view reveals expression in the hindbrain and spinal cord. **B:** *Scn1Lab* expression is detected in ventral regions of the hindbrain. **C:** Similarly, in the spinal cord, *scn1Lab* expression is detected in ventral regions (asterisks). **D:** Epifluorescent illumination of the Fast Red in situ hybridization signal reveals expression ventrally within the spinal cord (asterisks). **E:** Using the same hybridization conditions as for antisense, the sense probe does not reveal a signal. **F–J:** At 48 hpf, *scn1Lab* expression is found diffusely within rostral regions of the central nervous system. **F,G:** Within the rostral central nervous system, *scn1Lab* expression is detected diffusely within ventral regions. **H,I:** Within the spinal cord, *scn1Lab* expression appears weaker at 48 versus 24 hpf because it is only detected by epifluorescent (I, asterisks) and not brightfield (H) illumination. **J:** The sense probe does not reveal a signal at 48 hpf, even using epifluorescent illumination. as, antisense probe; n, notochord; s, sense probe; y, yolk sac; yse, yolk sac extension. Scale bars = 250  $\mu$ m in A (applies to A,F), 100  $\mu$ m in B (applies to B,G), 100  $\mu$ m in C (applies to C–E,H–J).

and developing dorsal root ganglion (Fig. 9I–L).

*Scn8ab* mRNA was found in a sub-

set of cells that express the *scn8aa*. At 24 hpf, transcripts were present in the trigeminal ganglia (Fig. 10A,B) and

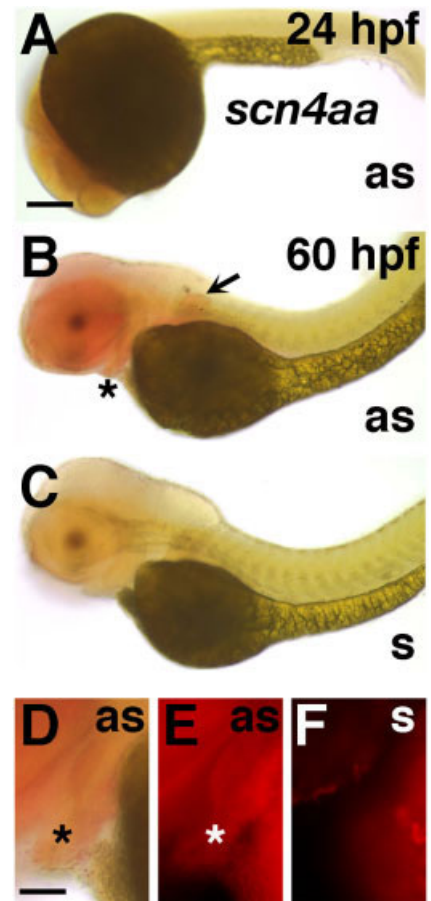


**Fig. 4.** *Scn4aa* is expressed in mesodermal tissues. **A:** At 24 hours postfertilization (hpf), *scn4aa* mRNA is barely detected dorsal to the yolk sac. **B:** At 72 hpf, transcripts are detected in head muscle, pharyngeal muscle (asterisk), and the pectoral fin (arrow). **C:** The sense probe does not reveal a signal. **D,E:** At 72 hpf, pharyngeal muscle expresses *scn4aa* mRNA. **F:** The sense probe does not reveal expression. Scale bars = 250  $\mu$ m in A (applies to A–C), 100  $\mu$ m in D (applies to D–F).

RB cells (Fig. 10C–E). Thus, in contrast to the other *scna* duplicated genes, *scn8aa* and *scn8ab* displayed overlapping expression patterns, with *scn8ab* present in a subset of cells that express *scn8aa*. For example, fewer RB cells expressed *scn8ab* versus *scn8aa*. At 60 hpf, similar to *scn8aa*, expression was detected within the lateral line system, albeit at lower levels (Fig. 11F,G). Unlike *scn8aa*, *scn8ab* was not expressed in the retina. In the spinal cord, as for *scn8aa*, *scn8ab* transcripts were present in both dorsal and ventral regions (Fig. 11H–J).

The data indicate that *scn8aa* is expressed in cell types that show reduced voltage-gated sodium current

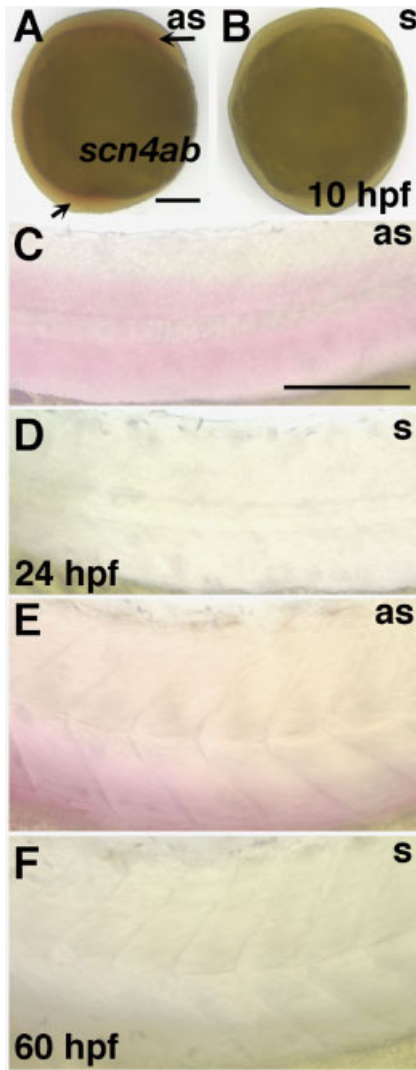


Fig. 5.

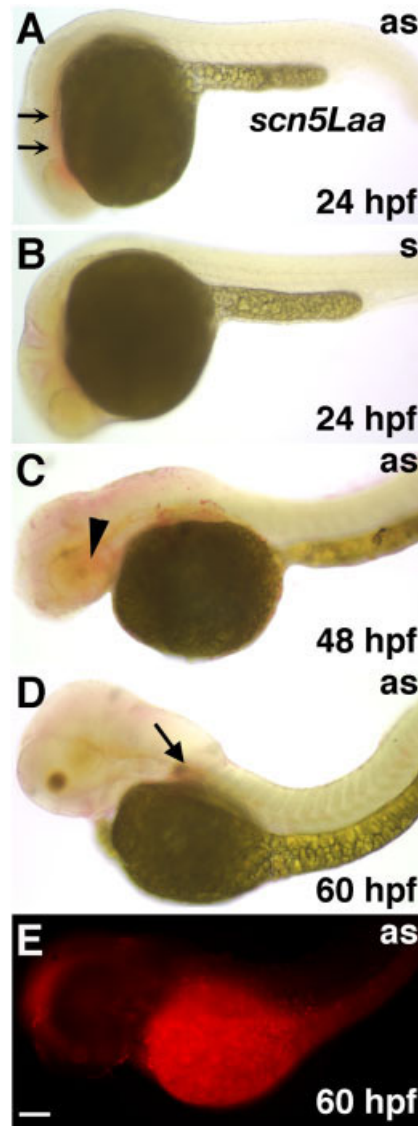


Fig. 6.

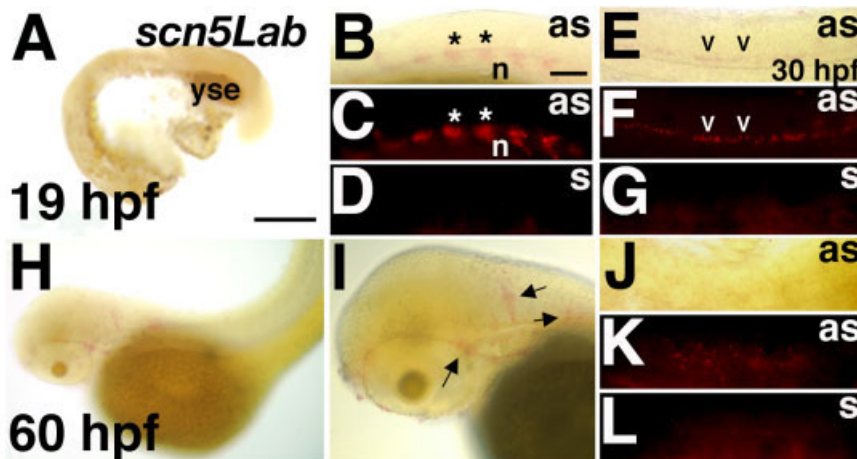


Fig. 7.

amplitudes in the mutant (Ribera and Nüsslein-Volhard, 1998; Gnügge et al., 2001). These data raise the possibility that the *mao* gene targets the *scn8aa*-encoded channel  $Na_v1.6a$ . In addition, our data provide new information regarding expression of *scn8ab*. However, the overlapping expression patterns of *scn8aa* and *scn8ab* do not provide obvious insights regarding the basis for retention of both genes in zebrafish.

### Novel Properties of the *scn8ab* Gene

In mammals, the *SCN8A* gene displays developmentally regulated splic-

**Fig. 5.** *Scn4ab* is expressed early in mesoderm and later in somatic tissue. **A,B:** At 10 hours postfertilization (hpf), *scn4ab* mRNA is detected in mesodermal tissue (arrows) using antisense but not sense probes. **C,D:** At 24 hpf, transcripts are detected in the trunk somites; in the dorsal somite, expression is most abundant in ventral region. **E,F:** At 60 hpf, expression is present in the somites and most abundantly in ventral half. Scale bars = 250  $\mu$ m in A (applies to A,B), 100  $\mu$ m in C (applies to C–F).

**Fig. 6.** In situ hybridization reveals neural expression of *scn5Laa*. **A:** At 24 hours postfertilization (hpf), *scn5Laa* mRNA is detected in regions associated with the developing heart tube and pharynx (arrows). **B:** Under the same conditions, the sense probe does not reveal a signal. **C:** At 48 hpf, *scn5Laa* expression shifts to more anterior and dorsal regions of the embryo (e.g., head muscle, arrowhead). **D,E:** At 60 hpf, *scn5Laa* expression appears in rostral regions of the central nervous system as well as the developing pectoral fin (arrow). Scale bars = 250  $\mu$ m in A (for A–E). as, antisense probe; s, sense probe.

**Fig. 7.** In situ hybridization reveals a temporally dynamic *scn5Lab* expression pattern. **A–D:** At 19 hours postfertilization (hpf), *scn5Lab* mRNA is detected in the developing somites of the trunk (asterisks in B,C). The in situ hybridization signal can be observed using either brightfield (B) or epifluorescent illumination (C). **E:** Under the same conditions, the sense probe does not reveal a signal. **E–G:** At 30 hpf, *scn5Lab* expression shifts from the peripheral somites to the central nervous system and is detected in ventral spinal cord (carats; E,F). **G:** The sense probe does not reveal a signal at 48 hpf, even using epifluorescent illumination. **H–L:** At 60 hpf, *scn5Lab* expression appears in the developing lateral line (I,L, arrows). In the trunk, expression is detected by epifluorescent (K) but not brightfield (J) illumination. **L:** The sense probe does not reveal a signal at 60 hpf, even using epifluorescent illumination. as, antisense probe; n, notochord; s, sense probe; yse, yolk sac extension. Scale bars = 250 and 100  $\mu$ m in A (applies to A & H and K, respectively), 100  $\mu$ m in B (applies to B–G,J–L).

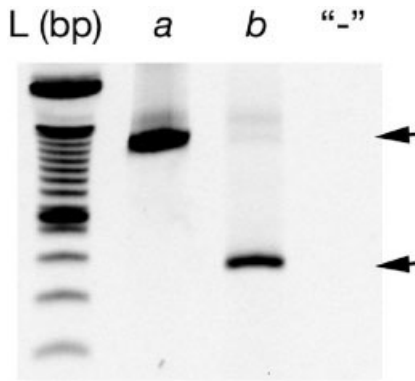


**Fig. 8. a,b:** Reverse transcriptase-polymerase chain reaction (RT-PCR) reveals expression of both *scn5Laa* (a) and *scn5Lab* (b) in heart tissue of 72 hours postfertilization (hpf) embryos. The negative control (-) consisted of RT-PCR using an RT reaction from which the enzyme had been omitted.

ing of exon 18 that codes for a region in transmembrane repeat III (Fig. 1; Plummer et al., 1997). Exon 18 has two variants: 18A and 18N (Table 3). The sequence of exon 18A predicts an open reading frame. In contrast, the sequence of exon 18N contains a stop codon that would result in a nonfunctional channel (Plummer et al., 1997). Neonatally, expression of exon 18N occurs as well as skipping of either exon 18 variant ( $\Delta 18$ ; Plummer et al., 1997). The developmental and/or physiological significance of this splicing pattern has not yet been established.

Because of the advantages of the zebrafish model for examination of embryonic development, we examined splicing of the exon 18 in *scn8aa* and *scn8ab*. Only one pattern of splicing is detected for *scn8aa* at any stage of development examined (Fig. 11). The size of the PCR product (512 bp) suggests that the transcripts contained the 18A-like exon. Direct sequencing of the PCR product confirmed this interpretation and indicated 84% identity at the nucleotide level with mouse exon 18A (Table 3).

In contrast, the *scn8ab* gene displayed developmentally regulated splicing of exon 18 (Fig. 11). Between 1 and 3 dpf, three PCR products are detected. The largest, 474 bp, corresponds to the size expected for inclusion of exon 18A. The two smaller bands, 421 and 351 bp, corresponded to inclusion of exon 18N and skipping

of exon 18, respectively. Direct sequencing of the PCR product confirmed this interpretation. Exons 18A and 18N of *scn8ab* are 79 and 27% identical to mouse exons 18A and 18N at the nucleotide level (Table 3).

It is possible that exon 18N for *scn8aa* might be present at other developmental stages not tested here. However, examination of genomic sequences suggests that this is unlikely. The zebrafish genomic databases ([http://www.ensembl.org/Danio\\_rerio/](http://www.ensembl.org/Danio_rerio/)) revealed exons 18A and 18N for *scn8ab*. In contrast, exon 18A but not 18N was detected for the *scn8aa* gene.

Thus, despite the minor differences between *scn8aa* and *scn8ab* with respect to primary sequences and expression patterns, the two genes differ substantially with respect to splicing of exon 18. *Scn8ab* but not *scn8aa* displays variants containing either exon 18N or no exon 18 ( $\Delta 18$ ). Furthermore, in both mammals and zebrafish, the inclusion of exon 18N and exclusion of exon 18 occurs during early developmental stages (Fig. 11; Plummer et al., 1997). In all species examined, the sequence of exon 18N includes a STOP codon, predicting a nonfunctional channel. Similarly, skipping of exon 18 also introduces a premature STOP codon, predicting a nonfunctional channel (Plummer et al., 1997). The experimental advantages of the zebrafish system (e.g., morpholino approaches) will allow examination of the physiological significance of embryonic expression of the exon 18 variants.

## CONCLUDING REMARKS

Comparison of zebrafish and mammalian SCNA expression patterns reveals substantial similarity for orthologous genes. The results suggest that *scna* expression may have been partitioned between duplicated genes in zebrafish. For example, *scn1Laa* and *scn1Lab* are thought to have evolved from the same ancestral gene as the mammalian *SCN1A*, *SCN2A*, *SCN3A*, and *SCN9A* genes (Novak et al., 2006). *Scn1Lab* was expressed in a manner resembling the combined expression patterns of *SCN1A*, *SCN2A*, and *SCN3A*. In contrast, *scn1Laa* and *SCN9A* displayed similar expression patterns. Similarly, *scn5Laa* and *scn5Lab* are evolutionar-

ily equally related to *SCN5A*, *SCN10A*, and *SCN11A*. Of interest, even though *scn5Laa* and *scn5Lab* displayed different expression patterns, both were expressed in tissues associated with the *SCN5A* expression pattern. However, neither is expressed in nociceptive-like sensory neurons, as are *SCN10A* and *SCN11A*. The latter result may indicate that such neurons do not appear in zebrafish until later stages of development or that processing of pain information in zebrafish differs significantly from that in mammals (see also, Lopreato et al., 2001).

Overall, the results indicate that *scna* gene expression occurs sufficiently early during zebrafish embryogenesis for sodium channels to play developmental roles, similar to calcium channels (Moran, 1991; Komuro and Rakic, 1992; Moreau et al., 1994; Drean et al., 1995; Leclerc et al., 1995, 1997, 2000; Palma et al., 2001; Rottbauer et al., 2001; Wallingford et al., 2001). The experimental strengths of the zebrafish model allow systematic analysis of the embryonic roles of each *scna* gene as well as specific splice variants.

## EXPERIMENTAL PROCEDURES

### Zebrafish

Fish were bred according to guidelines outlined in The Zebrafish Book (Westerfield, 1995). Embryos were raised at 28.5° and staged according to external morphological features as described by Kimmel et al. (1995).

### Whole-Mount In Situ Hybridization

Embryos and larvae, ranging in age between 10 and 120 hpf, were fixed in 4% paraformaldehyde in Fix buffer (4.0% sucrose, 0.15 mM  $\text{CaCl}_2$ , 0.1 M  $\text{PO}_4$ , pH 7.3; Westerfield, 1995), then dehydrated through a series of methanols, followed by a >24 hr incubation in 100% methanol (-20°C). Digoxigenin-labeled hybridization probes (Fig. 1) were synthesized by standard methods (Jowett, 1999). In situ hybridization was carried out as described by Schulte-Merker et al. (1992) with minor modifications. Detection of the anti-digoxigenin Fab-

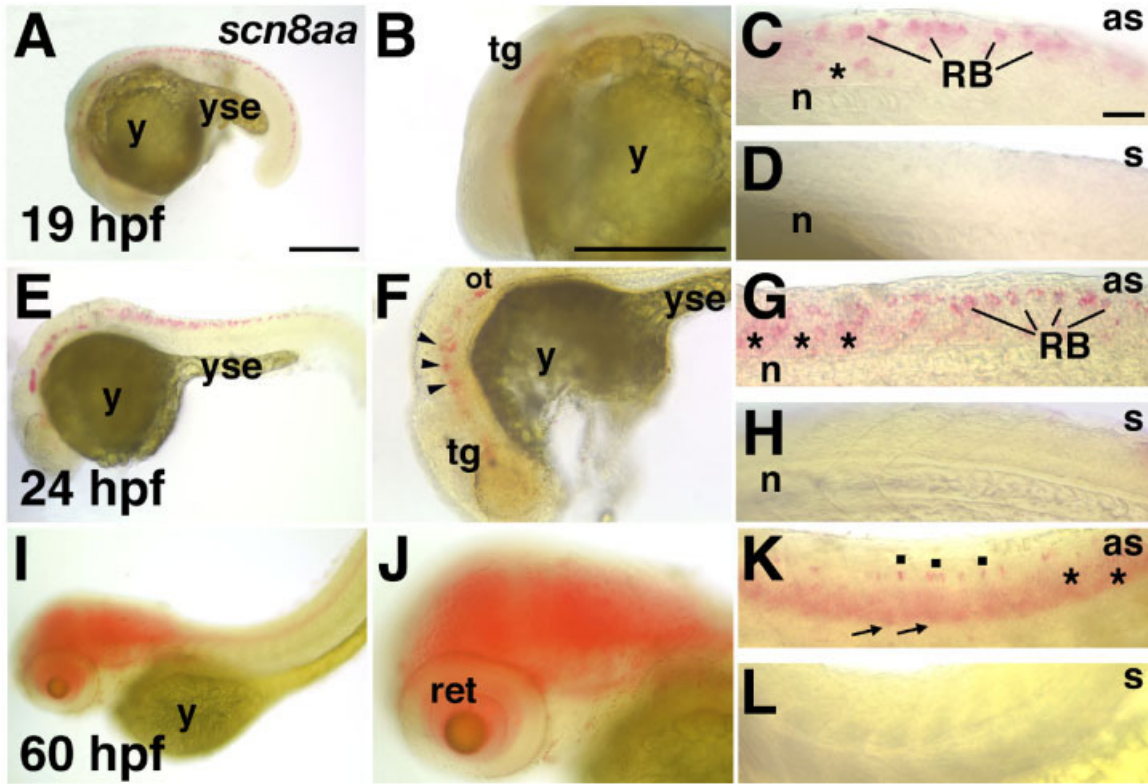


**Fig. 9.** *Scn8aa* expression is restricted to the nervous system. A–E: At 19 hours postfertilization (hpf), *scn8aa* mRNA is detected in the developing trigeminal ganglion and spinal cord. **A,B:** In anterior portions of the embryo, *scn8aa* mRNA is detected in the developing trigeminal ganglion (tg). **C:** In the spinal cord, *scn8aa* transcripts are detected dorsally in Rohon-Beard (RB) cells as well as ventrally (asterisk). **D:** Under the same conditions, the sense probe does not reveal a signal. E–H: At 24 hpf, *scn8aa* expression expands within the hindbrain. **E,F:** *scn8aa* transcripts are detected in ventral hindbrain at 24 hpf (arrowheads) and the trigeminal ganglion. **G:** In the spinal cord, *scn8aa* expression occurs in RB cells and diffusely in ventral regions. **H:** The sense probe does not reveal a signal at 24 hpf. I–L: At 60 hpf, *scn8aa* expression appears diffusely in both rostral and caudal regions of the central nervous system. **I,J:** In rostral regions of the central nervous system, *scn8aa* expression is detected in the retina and diffusely in the brain. **K:** In the spinal cord, expression is detected dorsally in isolated cells (dots) and more diffusely in ventral regions (asterisks). In addition, expression is detected in the periphery, in dorsal root ganglia (arrows). **L:** The sense probe did not reveal a signal at 60 hpf. as, antisense probe; n, notochord; ot, otic vesicle; ret, retina; s, sense probe; y, yolk sac; yse, yolk sac extension. Scale bars = 250  $\mu$ m in A (applies to A,E,I), 100  $\mu$ m in B (applies to B,F,J), 100  $\mu$ m in C (applies to C,D,G,H,K,L).

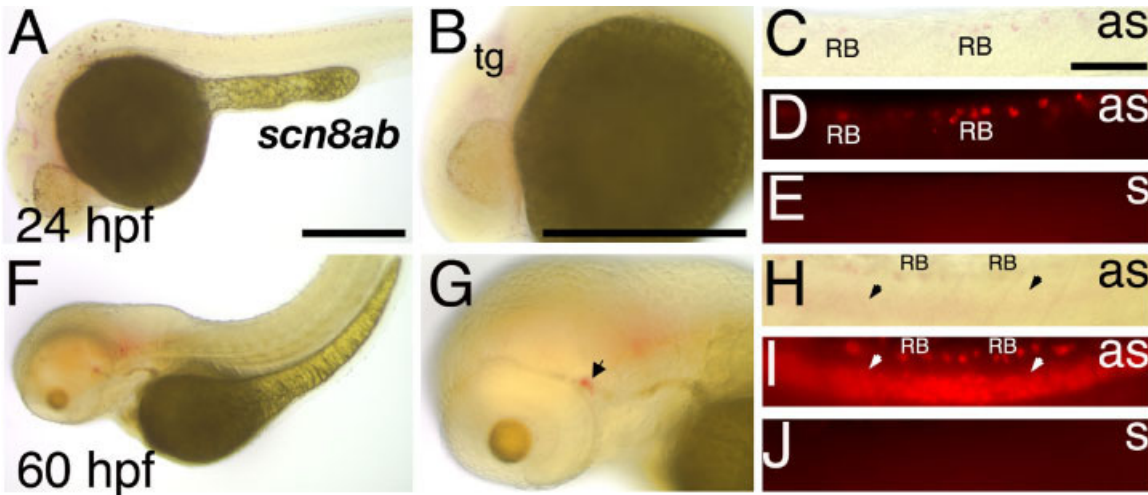


**Fig. 10.** *Scn8ab* transcripts are detected in a subset of the *scn8aa* expression domain. A–E: At 24 hours postfertilization (hpf), *scn8ab* mRNA is detected in the developing trigeminal ganglion and some Rohon-Beard (RB) cells. **A,B:** In anterior portions of the embryo, *scn8ab* mRNA is detected in developing trigeminal ganglion. **C,D:** In the spinal cord, *scn8ab* transcripts are detected in some but not all RB cells. **E:** Under the same conditions, the sense probe does not reveal a signal. F–J: At 60 hpf, *scn8ab* expression expands to ventral spinal cord. **F,G:** In anterior regions, *scn8ab* transcripts are detected in the lateral line system (arrow). **H,I:** In the spinal cord, *scn8ab* expression persists in some RB cells and is now present diffusely in ventral regions (arrowheads). **J:** The sense probe does not reveal a signal at 60 hpf. as, antisense probe; n, notochord; s, sense probe; tg, trigeminal ganglion; y, yolk sac; yse, yolk sac extension. Scale bars–250  $\mu$ m in A (applies to A,F), 250  $\mu$ m in B (applies to B,H), 100  $\mu$ m in C (applies to C–E,H–J).

alkaline phosphatase conjugated antibody was performed using the Fast Red chromogen (Sigma) and enhanced by the addition of NaCl to the staining solution (final 0.3 M; Chiu et al., 1996; Novak and Ribera, 2003). The Fast Red reaction was allowed to proceed for 5 to 24 hr, depending on mRNA abundance and probe efficacy. Embryos were washed for 2 hr in PBST, and the Fast Red reaction products were visualized with either bright field or epifluorescent optics.

Processed embryos were mounted laterally and viewed on an Eclipse TE200 inverted Nikon Microscope with a  $\times 20$  or  $\times 40$  objective and photographed by using a Princeton Instruments digital camera. Images were imported into Adobe PhotoShop for final figure preparation.

### Detection of *Scn5la* mRNAs in Larval Cardiac Tissue

RT was performed using Superscript II reverse transcriptase enzyme (GIBCO-

BRL, Gaithersburg, MD). RNA was isolated from 51 hearts isolated from 72 hpf larvae using the Trizol reagent. Two rounds of PCR were performed with the following primers (5'-3'): *scn5Laa*, F1: GCCTCACAATGTCTCAACACC, R1: GACTGACGATCAGACTGTGCGAC, R2: GGTTCGCTCAGGGCTCGGTC; *scn5Lab*, F1: CTCTCTGGACCAAATACCTCG, F2: GTACTGAGTGTTCACCTTCC, R1: CAGTCAAATCCATCAGGGCACT. The first PCR round used primers F1 and R1, 4  $\mu$ l of the RT product, and the following cycling parameters: 30 rounds at 95°C  $\times$  60 sec, 57  $\times$  30 sec, 72°C  $\times$  90 sec. The second nested PCR used primers F1 and R2 (*scn5Laa*) or F2 and R1 (*scn5Lab*) and 4  $\mu$ l of the first PCR with the following cycling parameters: 30 rounds at 95°C  $\times$  60 sec, 55  $\times$  60 sec, 72°C  $\times$  90 sec. The negative control tested for amplification of genomic DNA and consisted of using an "RT" reaction to which no reverse transcriptase had been added. PCR products were visualized by gel

electrophoresis and gel images were scanned and processed in Adobe PhotoShop.

### Analysis of *Scn8aa* and *Scn8ab* Splice Variants

RT-PCR was performed using RNA extracted from whole embryos at 24, 48, and 72 hpf using the Trizol reagent. RT was performed using Superscript II reverse transcriptase enzyme (GIBCO-BRL) with 2  $\mu$ g of total RNA random hexamer primers (Invitrogen). A single round of PCR (35 cycles) was performed using 1  $\mu$ l of RT product using forward (F) and reverse (R) primers that recognized sequences in Exons 17 (F) and 19 (R) that were specific for either *scn8aa* or *scn8ab* (*scn8aa*: F, 5'-TGAACAGAGGAAGACTATTCG-3', R, 5'-TTGACGTTCTTCCAACGCACC-3'; *scn8ab*: F, 5'-GAA-CAGAGGAAAACCATCCAG-3'; R, 5'-ATGAGTGCAAAGCATTCGGTC-3'). Cycling parameters for the PCR were as follows: 95°C  $\times$  60 sec, 51°C  $\times$  30 sec, 72°C  $\times$  120 sec. Negative controls consisted of using RT reactions to which no reverse transcriptase had been added. PCR products were visualized by gel electrophoresis and extracted and sequenced directly. Gel images were scanned and processed in Adobe PhotoShop.

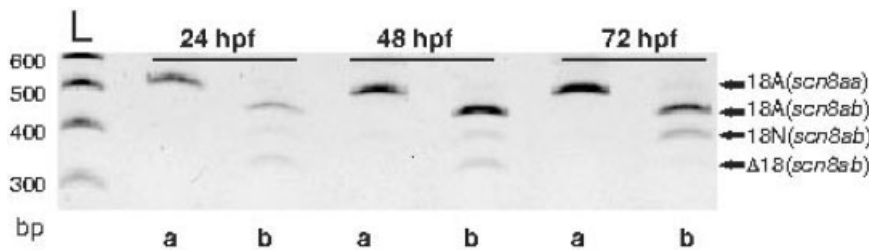


**Fig. 11.** Developmentally regulated splicing of exon 18 of *scn8ab* but not *scn8aa*. Reverse transcriptase-polymerase chain reaction was used to analyze splicing of exon 18 of both *scn8aa* and *scn8ab*. RNA was extracted from 24, 48, and 72 hours postfertilization (hpf) embryos. At all stages examined, *scn8aa* (lanes a) displayed only the 18A variant (512 bp). In contrast, *scn8ab* (lanes b) expresses three different variants: 18A (474 bp), 18N (421 bp), and  $\Delta$ 18 (351 bp).

### ACKNOWLEDGMENTS

We thank members of the Ribera laboratory for helpful suggestions and comments and Sarah Stroh for assistance with fish care.

**TABLE 3. Exons 18A and 18N<sup>a</sup>**

A. Exon 18A	
<i>SCN8A</i>	GTCTCTTTAGTCAGCCTTATAGCTAATGCCCTGGGCTACTCGGAAGTCTAGGTGCCATAAAGTCCCTTAGGACCCTAAGAGCTT
<i>scn8aa</i>	--G---A-----G-----C--T-----GC---T--A--A--C-----A-----G--CC
<i>scn8ab</i>	--G---A-----G-----A--CT-G--CC-----G--A--TT-G--G-----C
<i>SCN8A</i>	TGAGACCCTTAAGAGCCTTATCAGGATTTGAAGGGATGAGG
<i>scn8aa</i>	-----C-C-----A--G-----T-----
<i>scn8ab</i>	-C--G---C-G-----T--G--C--G-----G--C-----
B. Exon 18N	
<i>SCN8A</i>	GTTCCATTAAGTTGTCTGGCTTAATTTAATGGGAGCTTCT GG
<i>scn8ab</i>	TGC-G- --- -CACAGA--GCCT
<i>SCN8A</i>	GAGCTGCAGAC TGT AAAGGGCGAGG
<i>scn8ab</i>	---GG---T-AGAGGGCCGGGAAGTG-G---C---

<sup>a</sup>Dashes indicate identity with *Mus musculus* *SCN8A*. Spaces were introduced to enhance the alignment. The stop codons of both mouse and zebrafish exon 18N exons are underlined.

## REFERENCES

- Amores A, Force A, Yan YL, Joly L, Amemiya C, Fritz A, Ho RK, Langeland J, Prince V, Wang YL, Westerfield M, Ekker M, Postlethwait JH. 1998. Zebrafish hox clusters and vertebrate genome evolution. *Science* 282:1711–1714.
- Akopian AN, Sivilotti L, Wood JN. 1996. A tetrodotoxin-resistant voltage-gated sodium channel expressed by sensory neurons. *Nature* 379:257–262.
- Akopian AN, Souslova V, Sivilotti L, Wood JN. 1999a. Structure and distribution of a broadly expressed atypical sodium channel. *FEBS Lett* 400:183–187.
- Akopian AN, Souslova V, England S, Okuse K, Ogata N, Ure J, Smith A, Kerr BJ, McMahon SB, Boyce S, Hill R, Stanfa LC, Dickenson AH, Wood JN. 1999b. The tetrodotoxin-resistant sodium channel SNS has a specialized function in pain pathways. *Nat Neurosci* 2:541–548.
- Beckh S, Noda M, Lubbert H, Numa S. 1989. Differential regulation of three sodium channel messenger RNAs in the rat central nervous system during development. *EMBO J* 8:3611–3616.
- Black J, Yokoyama S, Higashida H, Ransom BR, Waxman SG. 1994. Sodium channel mRNAs I, II and III in the CNS: cell-specific expression. *Mol Brain Res* 22:275–289.
- Black J, Dib-Hajj S, McNabola K, Rizzo M, Waxman SG. 1996. Spinal sensory neurons express multiple sodium channel alpha-subunit mRNAs. *Brain Res Mol Brain Res* 43:117–131.
- Chiu KP, Sullivan T, Bursztajn S. 1996. Improved in situ hybridization: color intensity enhancement procedure for the alkaline phosphatase/Fast Red system. *Biotechniques* 20:964–966.
- Cooper KL, Armstrong J, Moens CB. 2005. Zebrafish foggy/spt 5 is required for migration of facial branchiomotor neurons but not for their survival. *Dev Dyn* 234:651–658.
- Cooperman SS, Grubman SA, Barchi RL, Goodman RH, Mandel G. 1987. Modulation of sodium-channel mRNA levels in rat skeletal muscle. *Proc Natl Acad Sci U S A* 84:8721–8725.
- Dib-Hajj SD, Tyrrell L, Black JA, Waxman SG. 1998. NaN, a novel voltage-gated Na channel, is expressed preferentially in peripheral sensory neurons and down-regulated after axotomy. *Proc Natl Acad Sci U S A* 95:8963–8968.
- Donahue LM, Coates PW, Lee VH, Ippensen DC, Arze SE, Poduslo SE. 2000. The cardiac sodium channel mRNA is expressed in the developing and adult rat and human brain. *Brain Res* 887:335–343.
- Drean G, Leclerc C, Duprat AM, Moreau M. 1995. Expression of L-type  $Ca^{2+}$  channel during early embryogenesis in *Xenopus laevis*. *Int J Dev Biol* 39:1027–1032.
- Escayg A, Heils A, MacDonald BT, Haug K, Sander T, Meisler MH. 2001. A novel SCN1A mutation associated with generalized epilepsy with febrile seizures plus—and prevalence of variants in patients with epilepsy. *Am J Hum Genet* 68:866–873.
- Felts PA, Yokoyama S, Dib-Hajj S, Black JA, Waxman SG. 1997. Sodium channel alpha-subunit mRNAs I, II, III, NaG, Na6 and hNE (PN1): different expression patterns in developing rat nervous system. *Brain Res Mol Brain Res* 45:71–82.
- Gellens ME, George AL Jr, Chen LQ, Chahine M, Horn R, Barchi RL, Kallen RG. 1992. Primary structure and functional expression of the human cardiac tetrodotoxin-insensitive voltage-dependent sodium channel. *Proc Natl Acad Sci U S A* 89:554–558.
- Gnügge L, Schmid S, Neuhauss SC. 2001. Analysis of the activity-deprived zebrafish mutant macho reveals an essential requirement of neuronal activity for the development of a fine-grained visuotopic map. *J Neurosci* 21:3542–3548.
- Goldin A. 2002. Evolution of voltage-gated  $Na^{+}$  channels. *J Exp Biol* 205:575–584.
- Granato M, van Eeden FJ, Schach U, Trowe T, Brand M, Furutani-Seiki M, Haffter P, Hammerschmidt M, Heisenberg CP, Jiang YJ, Kane DA, Kelsh RN, Mullins MC, Odenthal J, Nusslein-Volhard C. 1996. Genes controlling and mediating locomotion behavior of the zebrafish embryo and larva. *Development* 123:399–413.
- Hartmann HA, Colom LV, Sutherland ML, Noebels JL. 1999. Selective localization of cardiac SCN5A sodium channels in limbic regions of rat brain. *Nat Neurosci* 2:593–595.
- Hice RE, Moody WJ. 1988. Fertilization alters the spatial distribution and the density of voltage-dependent sodium current in the egg of the ascidian *Bolitena villosa*. *Dev Biol* 127:408–420.
- Higashijima S, Hotta Y, Okamoto H. 2000. Visualization of cranial motor neurons in live transgenic zebrafish expressing green fluorescent protein under the control of the islet-1 promoter/enhancer. *J Neurosci* 20:206–218.
- Hille B. 2001. Ion channels of excitable membranes. 3rd ed. Sunderland, MA: Sinauer Associates, Inc.
- Jowett T. 1999. Analysis of protein and gene expression. *Methods Cell Biol* 59:63–85.
- Kallen RG, Sheng ZH, Yang J, Chen LQ, Rogart RB, Barchi RL. 1990. Primary structure and expression of a sodium channel characteristic of denervated and immature rat skeletal muscle. *Neuron* 4:233–242.
- Kimmel CB, Ballard WW, Kimmel SR, Uhlmann B, Schilling TF. 1995. Stages of embryonic development of the zebrafish. *Dev Dyn* 203:253–310.
- Komuro H, Rakic P. 1992. Selective role of N-type calcium channels in neuronal migration. *Science*. 257:806–809.
- Krzemien D, Schaller K, Levinson SR, Caldwell J. 2000. Immunolocalization of sodium channel isoform NaCh6 in the nervous system. *J Comp Neurol* 420:70–83.
- Leclerc C, Duprat AM, Moreau M. 1995. In vivo labeling of L-type  $Ca^{2+}$  by fluorescent dihydropyridine: correlation between ontogenesis of the channels and the acquisition of neural competence in ectoderm cells from *Pleurodeles waltl* embryos. *Cell Calcium* 17:216–224.
- Leclerc C, Daguzan C, Nicolas MT, Chabret C, Duprat AM, Moreau M. 1997. L-type calcium channel activation controls the in vivo transduction of the neuralizing signal in the amphibian embryos. *Mech Dev* 64:105–110.
- Leclerc C, Webb SE, Daguzan C, Moreau M, Miller AL. 2000. Imaging patterns of calcium transients during neural induction in *Xenopus laevis* embryos. *J Cell Sci* 113:3519–3529.
- Lopreato GF, Lu Y, Southwell A, Atkinson NS, Hillis DM, Wilcox TP, Zakon HH. 2001. Evolution and divergence of sodium channel genes in vertebrates. *Proc Natl Acad Sci U S A* 98:7588–7592.
- Moran D. 1991. Voltage-dependent L-type  $Ca^{2+}$  channels participate in regulating neural crest migration and differentiation. *Am J Anat* 192:14–22.
- Moreau M, Leclerc C, Gualandris-Parisot L, Duprat AM. 1994. Increased internal  $Ca^{2+}$  mediates neural induction in the amphibian embryo. *Proc Natl Acad Sci U S A* 91:12639–12643.
- Neuhauss SC, Biehlermaier O, Seeliger MW, Das T, Kohler K, Harris WA, Baier H. 1999. Genetic disorders of vision revealed by a behavioral screen of 400 essential loci in zebrafish. *J Neurosci* 19:8603–8615.
- Noda M, Ikeda T, Kayano T, Suzuki H, Takeshima H, Kurasaki M, Takahashi H, Numa S. 1986. Existence of distinct sodium channel messenger RNAs in rat brain. *Nature* 320:188–192.
- Novak AE, Ribera AB. 2003. Immunocytochemistry as a tool for zebrafish developmental neurobiology. *Methods Cell Sci* 25:79–83.
- Novak AE, Ribera AB. 2005. The zebrafish embryo as an integrative physiology model system. In: Walz W, editor. Integrative physiology: in the proteomics and post-genomics age. Totowa, NJ: Humana Press.
- Novak AE, Jost MC, Lu Y, Taylor AD, Zakon HH, Ribera AB. 2006. Gene duplications and evolution of vertebrate voltage-gated sodium channels. *J Mol Evol* (under second review).
- Nüsslein-Volhard C, Dahm R. 2002. Zebrafish: A Practical Approach. Oxford University Press, Oxford, England.
- Palma V, Kukuljan M, Mayor R. 2001. Calcium mediates dorsoventral patterning of mesoderm in *Xenopus*. *Curr Biol* 11:1606–1610.
- Plummer NW, McBurney MW, Meisler MH. 1997. Alternative splicing of the sodium channel SCN8A predicts a truncated two-domain protein in fetal brain and non-neuronal cells. *J Biol Chem* 272:24008–24015.

- Plummer NW, Meisler MH. 1999. Evolution and diversity of mammalian sodium channel genes. *Genomics* 57:323–331.
- Postlethwait J, Amores A, Cresko W, Singer A, Yan YL. 2004. Subfunction partitioning, the teleost radiation and the annotation of the human genome. *Trends Genet* 20:481–490.
- Raible DW, Kruse GJ. 2000. Organization of the lateral line system in embryonic zebrafish. *J Comp Neurol* 421:189–198.
- Renganathan M, Dib-Hajj S, Waxman SG. 2002. Na(v)1.5 underlies the 'third TTX-R sodium current' in rat small DRG neurons. *Brain Res Mol Brain Res* 106:70–82.
- Ribera A, Nüsslein-Volhard C. 1998. Zebrafish touch-insensitive mutants reveal an essential role for the developmental regulation of sodium current. *J Neurosci* 18:9181–9191.
- Rogart RB, Cribbs LL, Muglia LK, Kephart DD, Kaiser MW. 1989. Molecular cloning of a putative tetodotoxin-resistant rat heart Na<sup>+</sup> channel isoform. *Proc Natl Acad Sci U S A* 86:8170–8174.
- Rottbauer W, Baker K, Wo ZG, Mohideen MA, Cantiello HF, Fishman MC. 2001. Growth and function of the embryonic heart depend upon the cardiac-specific L-type calcium channel alpha1 subunit. *Dev Cell* 1:265–275.
- Rutenberg J, Cheng SM, Levin M. 2002. Early embryonic expression of ion channels and pumps in chick and *Xenopus* development. *Dev Dyn* 225:469–484.
- Schaller KL, Caldwell JH. 2000. Developmental and regional expression of sodium channel isoform NaCh6 in the rat central nervous system. *J Comp Neurol* 420:84–97.
- Schaller KL, Krzemien DM, Yarowsky PJ, Krueger BK, Caldwell JH. 1995. A novel, abundant sodium channel expressed in neurons and glia. *J Neurosci* 15:3231–3242.
- Schultel-Merker S, Ho RK, Herrmann BG, Nusslein-Volhard C. 1992. The protein product of the zebrafish homologue of the mouse T gene is expressed in nuclei of the germ ring and the notochord of the early embryo. *Development* 116:1021–1032.
- Svoboda KR, Linares AE, Ribera AB. 2001. Activity regulates programmed cell death of zebrafish Rohon-Beard neurons. *Development* 128:3511–3520.
- Toledo-Aral JJ, Moss BL, He ZJ, Koszowski AG, Whisenand T, Levinson SR, Wolf JJ, Silos-Santiago I, Halegoua S, Mandel G. 1997. Identification of PN1, a predominant voltage-dependent sodium channel expressed principally in peripheral neurons. *Proc Natl Acad Sci U S A* 94:1527–1532.
- Trimmer JS, Cooperman SS, Tomiko SA, Zhou JY, Crean SM, Boyle MB, Kallen RG, Sheng ZH, Barchi RL, Sigworth FJ, Goodman RH, Agnew WS, Mandel G. 1989. Primary structure and functional expression of a mammalian skeletal muscle sodium channel. *Neuron* 3:33–49.
- Trimmer JS, Cooperman SS, Agnew WS, Mandel G. 1990. Regulation of muscle sodium channel transcripts during development and in response to denervation. *Dev Biol* 142:360–367.
- Tsai CW, Tseng JJ, Lin SC, Chang CY, Wu JL, Horng JF, Tsay HJ. 2001. Primary structure and developmental expression of zebrafish sodium channel Na(v)1.6 during neurogenesis. *DNA Cell Biol* 20:249–255.
- Wallingford JB, Harland R, Fraser S. 2001. Calcium signaling during convergent extension in *Xenopus*. *Curr Biol* 11:652–661.
- Weiss LA, Escayg A, Kearney JA, Trudeau M, MacDonald BT, Mori M, Reichert J, Buxbaum JD, Meisler MH. 2003. Sodium channels SCN1A, SCN2A and SCN3A in familial autism. *Mol Psychiatry* 8:186–194.
- Westerfield M. 1995. *The zebrafish book: a guide for the laboratory use of zebrafish (Brachydanio rerio)*. Eugene, OR: University of Oregon Press.
- Yang JS, Sladky JT, Kallen RG, Barchi RL. 1991. TTX-sensitive and TTX-insensitive sodium channel mRNA transcripts are independently regulated in adult skeletal muscle after denervation. *Neuron* 7:421–427.